

Diffusion of Temporal Field Correlation with Selected Applications

D. A. Boas*[†], I. V. Meglinsky^{†‡}, L. Zemaný*, L. E. Campbell*[®], B. Chance[†],
and A. G. Yodh*

*Department of Physics,

[†]Department of Biophysics and Biochemistry,
University of Pennsylvania, Philadelphia, PA 19104

[‡] Department of Optics, Saratov State University, Saratov, 410071 Russia

[®] Present address Department of Physics, Hobart and William Smith Colleges,
Geneva, NY 14456

ABSTRACT

We consider the transport of the electric field temporal autocorrelation in *heterogeneous*, fluctuating turbid media. Experiments are performed in strongly scattering media with spatially separated static and dynamic components, and low resolution "dynamical" images of such media are obtained using autocorrelation measurements of the emerging speckle fields taken along the sample surface. Our analysis, based on a diffusion approximation to the field correlation transport equation, reveals that the field correlation scatters from macroscopic dynamical heterogeneities within turbid media. Demonstrations using heterogeneous samples containing particles undergoing Brownian motion and shear flow are described.

Keywords: Photon Diffusion, Diffusing-Wave Spectroscopy, Optical Imaging, Correlations, Brownian Motion, Flow

1 Introduction

For many years the temporal fluctuations of light fields have been used to extract dynamical information about material motions. Most experiments of this nature¹⁻³ are carried out in optically thin materials which scatter incident photons no more than once. More recently however, there has been a growing interest in the properties of light fields emerging from turbid media.⁴⁻⁶ The most robust of these phenomena are associated with light fields that diffuse through turbid media in a manner similar to heat flow. A beautiful example of these developments is the technique of diffusing-wave spectroscopy,^{5,6} where the temporal correlation functions of the emerging diffuse speckle fields have provided fundamental new information about motions in *homogeneous* turbid colloids,⁷ foams,⁸ and emulsions.⁹ Parallel developments have occurred in the biophysics community where simpler properties of diffusing photons, such as the scattering of diffuse photon density waves, are presently used to generate low resolution images of stationary absorption and scattering variations within heterogeneous tissues.⁴

In this paper we consider the diffusion of temporal field correlation through *heterogeneous* turbid media. The work presented here constitutes a modest extension of some of our early work that has already appeared in the literature.¹⁰ We show that the transport of diffusive temporal field correlation through a medium consisting of spatially distinct static and dynamic parts, can be viewed as a scattering process, and we experimentally

demonstrate that position-dependent measurements of the diffusing light field temporal autocorrelation function can be used to reconstruct images of the spatial variation of *dynamical* properties within the medium. Besides its intrinsic interest as a new phenomenon, the scattering of diffusive temporal field correlation offers an unexplored contrast mechanism for imaging within heterogeneous turbid media such as tissue, and provides experimenters with a better framework for the interpretation of correlation functions from more complex, spatially heterogeneous biological samples, colloids, foams, and emulsions. In our previous paper,¹⁰ we presented the correlation diffusion equation and experimental results for systems with dynamics governed by Brownian motion. In the current chapter we review the previous results, experimentally demonstrate the validity of our approach for systems with flow, and describe in more detail the derivation of the correlation diffusion equation starting from the correlation transport equation.

2 Correlation Diffusion Theory

The temporal field autocorrelation function of coherent light emanating from a scattering medium provides information about the dynamics of the medium. The reader is referred to reviews on quasi-elastic light scattering (QELS) for an analysis of correlation functions in the single scattering regime.¹⁻³ In the present paper we are interested in the field autocorrelation function of multiply scattered light.

The normalized temporal electric field autocorrelation function, $g_1(\tau)$, of light that has diffused through a *homogeneous* turbid colloid has been determined and, within the framework of DWS,⁶ is given by

$$g_1(\tau) = \frac{\langle E(t)E^*(t+\tau) \rangle}{\langle |E|^2 \rangle} = \int_0^\infty ds P(s) \exp(-2\mu'_s D_B k_o^2 \tau s). \quad (1)$$

Here, $E(t)$ is the electric field of the emerging speckle at time t , τ is the correlation time delay, $P(s)$ is the probability that a photon will travel a length s between the source and detector, D_B is the translational diffusion coefficient of the scattering particles, k_o is the wavenumber of the photon in the medium, and μ'_s is the reduced scattering factor for the diffusing photon. The brackets denote an ensemble average which, for an ergodic system, is the same as a temporal average. This form for the temporal field autocorrelation function is accurate for homogeneous, fluctuating turbid media, such as colloids, but cannot be easily extended to encompass heterogeneous systems. Here, homogeneous refers to the absorption, scattering, and *dynamical* properties of the medium.

The theoretical basis of our approach for *heterogeneous* systems may be derived from the linear transport equation for field correlation recently presented by Ackerson *et al.*¹¹ or by field theoretic methods.⁵ Both methods are valid for scalar fields. In this paper, we derive the correlation diffusion equation from the correlation transport equation using the P_1 approximation.¹³⁻¹⁶

The linear transport equation for correlation presented by Ackerson *et al.*¹¹ is analogous to the transport equation for photons. The primary distinction is that the transport equation for correlation considers the dynamical processes that decorrelate the phase of the electric field. The steady state correlation transport equation is

$$\nabla \cdot G_1(\mathbf{r}, \hat{s}, \tau) \hat{s} + \mu_t G_1(\mathbf{r}, \hat{s}, \tau) = \mu_s \int_{4\pi} G_1(\mathbf{r}, \hat{s}', \tau) g_1^s(\hat{s}, \hat{s}', \tau) f(\hat{s}, \hat{s}') ds' + Q(\mathbf{r}, \hat{s}). \quad (2)$$

Here, $G_1(\mathbf{r}, \hat{s}, \tau)$ is the *unnormalized* temporal field-autocorrelation function (i.e. $G_1(\mathbf{r}, \hat{s}, \tau) = \langle E(0)E^*(\tau) \rangle$ and has units of intensity, photons per area per second) which is a function of position \mathbf{r} , direction \hat{s} , and correlation time τ . The photon scattering and absorption coefficients are respectively μ_s and μ_a , and $\mu_t = \mu_s + \mu_a$. The integral is over all directions s' and thus accounts for the scattering of photons from direction s' to s using the phase function $f(\hat{s}, \hat{s}')$ and the *normalized* temporal field autocorrelation function for *single scattering* $g_1^s(\hat{s}, \hat{s}', \tau)$. In the case of particles undergoing Brownian motion

$$g_1^s(\hat{s}, \hat{s}', \tau) = \exp \left[-2D_B K_o^2 \tau (1 - \hat{s}' \cdot \hat{s}) \right]. \quad (3)$$

Finally, v is the speed of light in the medium and $Q(\mathbf{r}, \hat{s})$ is the distribution of light sources with units of photons per volume per second. Note that when $\tau = 0$, the steady state correlation transport equation is reduced to the steady state photon transport equation (see, for example, books by Ishimaru,¹² Case and Zweifel,¹³ Davison and Sykes,¹⁴ and Glasstone and Edlund¹⁵ for discussions of the transport equation).

The correlation transport equation, eq. (2), is valid as long as photon localization effects are negligible. Eq. (2) is essentially a conservation equation for temporal field correlation. The left-hand side accounts for the flux, scattering, and absorption of correlation from a point in the six dimensional phase-space. This loss of correlation from a point in phase-space is balanced by the gain as given on the right-hand side. The first term of the right-hand side accounts for the scattering of correlation from all directions at position \mathbf{r} into the particular direction given by the point in the six dimensional phase-space, while the second term is simply the source of photons at that point in phase-space.

Within the P_1 approximation,¹³⁻¹⁵ the correlation transport equation reduces to the following steady-state diffusion equation (details of the derivation are provided in the appendix),

$$\left(D_\gamma \nabla^2 - v\mu_a - 2v\mu'_s D_B k_o^2 \tau \right) G_1(\mathbf{r}, \tau) = -vS(\mathbf{r}), \quad (4)$$

where $D_\gamma = \frac{v}{3\mu'_s}$ is the *photon diffusion coefficient*. Notice that in the correlation diffusion equation, $G_1(\mathbf{r}, \tau)$ is no longer a function of \hat{s} and the reduced scattering coefficient, μ'_s , appears instead of the scattering coefficient, μ_s , and the normalized differential phase function. Also the source, $S(\mathbf{r})$, has been assumed isotropic.

Eq. (4) can be recast as a Helmholtz equation for the field correlation function, i.e.

$$\left(\nabla^2 + K^2(\tau) \right) G_1(\mathbf{r}, \tau) = -\frac{vS}{D_\gamma} \delta^3(\mathbf{r} - \mathbf{r}_s), \quad (5)$$

where $K^2(\tau) = -3\mu'_s(\mu_a + 2\mu'_s D_B k_o^2 \tau)$. Here we have taken the light source to be point-like and located at position \mathbf{r}_s . Note that $2\mu'_s D_B k_o^2 \tau$ is a loss term similar to μ_a . While μ_a represents losses due to photon absorption, $2\mu'_s D_B k_o^2 \tau$ represents the "absorption" of correlation due to dynamical processes. When $\tau = 0$ there is no dynamical absorption and eq. (5) reduces to the steady-state photon diffusion equation.⁴

For an infinite, homogeneous system with no photon absorption (i.e. $\mu_a = 0$), the solution to eq. (5) has the well known form $G_1(\mathbf{r}, \tau) = vS \exp(-\sqrt{6\mu'_s D_B k_o^2 \tau} |\mathbf{r} - \mathbf{r}_s|) / (4\pi D_\gamma |\mathbf{r} - \mathbf{r}_s|)$. The same solution has been derived from the scalar wave equation for the electric field propagating in a medium with a fluctuating dielectric constant,⁵ and within the context of diffusing-wave spectroscopy.⁶ In contrast to these two approaches, the correlation diffusion equation provides a simple framework for considering turbid media with large scale *spatially varying dynamics*, that is, media where $D_B = D_B(\mathbf{r})$.

The correlation diffusion equation derived here is for turbid samples with dynamics governed by Brownian motion. The correlation diffusion equation can be modified to account for other dynamical processes. In the cases of random flow and shear flow the correlation diffusion equation becomes

$$\left(D_\gamma \nabla^2 - v\mu_a - 2v\mu'_s D_B k_o^2 \tau - \frac{1}{3} v\mu'_s \langle V^2 \rangle k_o^2 \tau^2 - \frac{1}{15} v\mu'_s \Gamma_{eff}^2 k_o^2 \tau^2 \right) G_1(\mathbf{r}, \tau) = -vS(\mathbf{r}). \quad (6)$$

The fourth and fifth terms on the left-hand side of eq. (6) arise from random and shear flows respectively. $\langle V^2 \rangle$ is the second moment of the particle speed distribution (assuming the velocity distribution is isotropic and gaussian),¹⁷ and Γ_{eff} is the effective shear rate.¹⁸ Notice that the "dynamical absorption" for flow in eq. (6) increases as τ^2 (compared to the τ increase for Brownian motion) because particles in flow fields travel ballistically; also D_B , $\langle V^2 \rangle$, and Γ_{eff} appear separately because the different dynamical processes are uncorrelated. The form of the "dynamical absorption" term for random flow is related to that for Brownian motion. Both are of the form $\frac{1}{3} v\mu'_s \langle \Delta r^2(\tau) \rangle$, where $\langle \Delta r^2(\tau) \rangle$ is the mean square displacement of a scattering particle. For Brownian

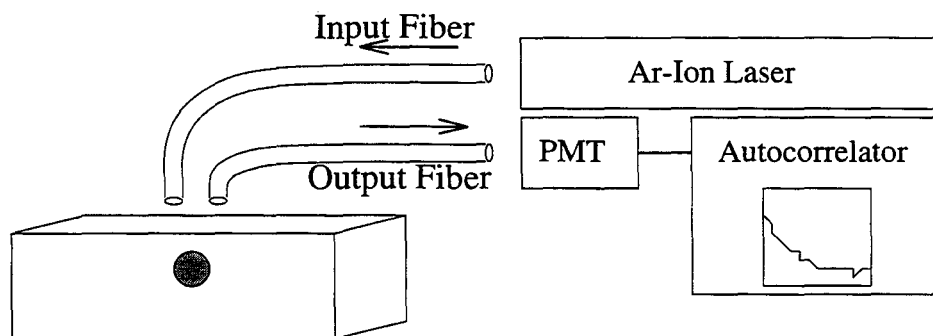


Figure 1: The 514 nm line from an argon ion laser (operated at 2.0 W with an etalon) is coupled into a multi-mode fiber optic cable and delivered to the surface of a solid slab of TiO_2 suspended in resin. The slab has dimensions of 15x15x8 cm. A spherical cavity with a diameter of 2.5 cm is located 1.8 cm below the center of the upper surface. The cavity is filled with a 0.2% suspension of 0.296 μm diameter polystyrene spheres at 25 °C resulting in $\mu'_s = 6.67 \text{ cm}^{-1}$, $\mu_a = 0.002 \text{ cm}^{-1}$, and $D_B = 1.5 \times 10^{-8} \text{ cm}^2 \text{ s}^{-1}$. For the solid, $\mu'_s = 4.54 \text{ cm}^{-1}$ and $\mu_a = 0.002 \text{ cm}^{-1}$. A single-mode fiber collects light at a known position and delivers it to a photo-multiplier tube (PMT), whose output enters a digital autocorrelator to obtain the temporal intensity correlation function. The temporal intensity correlation function is related to the temporal field correlation function by the Siegert relation⁶. The fibers can be moved to any position on the sample surface.

motion $\langle \Delta r^2(\tau) \rangle = 6D_B\tau$ and for random flow $\langle \Delta r^2(\tau) \rangle = \langle V^2 \rangle \tau^2$. The derivation of the "dynamical absorption" term for shear flow is more complex and the reader is referred to Wu *et al.*¹⁸ for a complete discussion. A detailed derivation of eq. (6) will be given in a future publication.

Flow in turbid media is an interesting problem that has received some attention. In these measurements experimenters typically determine a correlation function that may be a compound of many decays representing a weighted average of flow within the sample. For example, Bonner and Nossal have developed an approach for measuring random blood flow in homogeneous tissue,¹⁷ Wu *et al.* have applied DWS to study uniform shear flow,¹⁸ and Bicout and co-workers have applied DWS to study inhomogeneous flow and turbulence.¹⁹ In all cases, *a priori* knowledge of the flow is used in the analyses. We expect that the application of correlation diffusion imaging will further clarify information about heterogeneous flows in turbid media.

3 Correlation Diffusion in Heterogeneous Systems

In this section we will review three solutions of the diffusion equation in heterogeneous systems. The first two are analytic solutions for an otherwise infinite homogeneous system containing a spherical or cylindrical heterogeneity, while the third is a more general perturbative method. These solutions are easily modified for semi-infinite media by satisfying the extrapolated zero boundary condition.²⁰

3.1 Exact Solution for Spherical Inhomogeneities

For piecewise homogeneous media, a solution to the diffusion equation is found by requiring that the differential equation in each homogeneous region is satisfied while matching the boundary conditions at the surface between

regions. An analytic solution exists for a medium which is homogeneous in all respects except for a spherical region (with radius a) characterized by a different value of D_B , μ'_s , and/or μ_a from the surrounding medium. The analytic solution of the correlation diffusion equation for this system reveals that the measured correlation function outside the sphere can be interpreted as a superposition of the incident/background correlation plus a term which accounts for the scattering of the correlation from the sphere, i.e.

$$G_1^{out}(\mathbf{r}_s, \mathbf{r}_d, \tau) = \frac{vS \exp(iK^{out}|\mathbf{r}_d - \mathbf{r}_s|)}{4\pi D_\gamma |\mathbf{r}_d - \mathbf{r}_s|} + \sum_{l=0}^{\infty} A_l h_l^{(1)}(K^{out}r_d) Y_l^0(\theta, \phi). \quad (7)$$

Here, $h_l^{(1)}(x)$ are Hankel functions of the first kind and $Y_l^0(\theta, \phi)$ are spherical harmonics.²¹ The coefficient A_l is found by matching the appropriate boundary conditions on the surface of the sphere. These boundary conditions are the same as for photon diffusion, namely the correlation is continuous ($G_1^{out}(\mathbf{r}, \tau) = G_1^{in}(\mathbf{r}, \tau)$) and the normal flux of correlation is continuous ($-D_\gamma^{out} \hat{n} \cdot \nabla G_1^{out}(\mathbf{r}, \tau) = -D_\gamma^{in} \hat{n} \cdot \nabla G_1^{in}(\mathbf{r}, \tau)$) across the surface of the sphere ($G_1^{in}(\mathbf{r}, \tau)$ is the correlation function inside the spherical object and \hat{n} is the normal vector to the sphere). Applying these boundary conditions, we find

$$A_l = \frac{-ivSK^{out}}{D_\gamma^{out}} h_l^{(1)}(K^{out}z_s) Y_l^{0*}(\pi, 0) \left[\frac{D_\gamma^{out} x j_l'(x) j_l(y) - D_\gamma^{in} y j_l(x) j_l'(y)}{D_\gamma^{out} x h_l^{(1)'}(x) j_l(y) - D_\gamma^{in} y h_l^{(1)}(x) j_l'(y)} \right], \quad (8)$$

where j_l are the spherical Bessel functions of the first kind, $x = K^{out}a$, $y = K^{in}a$, a is the radius of the sphere, \mathbf{r}_s is the position of the source,²¹ and j_l' and $h_l^{(1)'}$ are the first derivatives of the functions j_l and $h_l^{(1)}$ with respect to the argument. This solution has been discussed in detail for diffuse photon density waves.²²

By viewing the perturbation of temporal correlation as a scattering process, simple algorithms adapted from scattering theory can be applied to reconstruct images of spatially varying dynamics in turbid media.

3.2 Exact Solution for Cylindrical Inhomogeneities

The derivation of the analytic solution for a cylinder is similar to that for a sphere. Once again, the correlation is a superposition of the incident and scattered correlation, i.e. $G_1^{out} = G_1^o + G_1^{scatt}$. For a cylinder of infinite length, the solution for the scattered wave in cylindrical coordinates is²³

$$G_1^{scatt}(r, \theta, z) = -\frac{vS}{2\pi^2 D_\gamma} \sum_{n=1}^{\infty} \int_0^{\infty} dp \cos(n\theta) \cos(pz) \\ \times K_n(\sqrt{p^2 - (K^{out})^2} r) K_n(\sqrt{p^2 - (K^{out})^2} r_s) \\ \times \left[\frac{D_\gamma^{out} x I_n'(x) I_n(y) - D_\gamma^{in} y I_n(x) I_n'(y)}{D_\gamma^{out} x K_n I(x) I_n(y) - D_\gamma^{in} y K_n(x) I_n'(y)} \right], \quad (9)$$

where I_n and K_n are modified Bessel functions, $x = \sqrt{p^2 - (K^{out})^2} a$, $y = \sqrt{p^2 - (K^{in})^2} a$, and a is the radius of the cylinder. The solution has been simplified by taking the z -axis as the axis of the cylinder and assuming that the source is at $z = 0$ and $\theta = 0$.

3.3 Rytov Approximation for General Inhomogeneities

For a system with a spatially varying particle self-diffusion coefficient, we approximate the correlation diffusion equation as

$$\left(\nabla^2 + K^2(\mathbf{r}, \tau) \right) G_1(\mathbf{r}, \tau) = -\frac{vS}{D_\gamma} \delta^3(\mathbf{r} - \mathbf{r}_s), \quad (10)$$

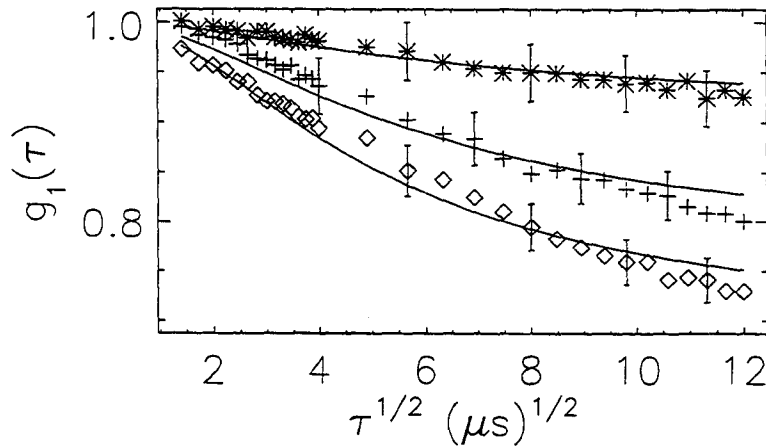


Figure 2: Experimental measurements of the normalized temporal field autocorrelation function for three different source-detector pairs are compared with the analytic solution for correlation scattering from a sphere. With respect to an x-y coordinate system whose origin lies directly above the center of the spherical cavity, the source-detector axis was aligned parallel to the y-axis with the source at $y=1.0$ cm and the detector at $y=-0.75$ cm. Keeping the source-detector separation fixed at 1.75 cm, measurements were made at $x=0.0$ cm, 1.0 cm, and 2.0 cm, and are indicated by the \diamond 's, + 's, and * 's respectively. The uncertainty for these measurements is 3% and arises from uncertainty in the position of the source and detector. The solid line was calculated using the known experimental parameters (see fig. 1). Note that larger and more rapid decays are observed when the source and detector are nearest the dynamic sphere. Here the largest fraction of detected photons have sampled the dynamic region.

where $K^2(\mathbf{r}, \tau) = -3\mu'_s(\mu_a + 2\mu'_s D_B(\mathbf{r})k_o^2\tau)$ and $D_B(\mathbf{r}) = D_B^{avg} + \delta D_B(\mathbf{r})$. The average particle self-diffusion coefficient of the system is given by D_B^{avg} ; $\delta D_B(\mathbf{r})$ represents the position dependent variation of $D_B(\mathbf{r})$ with respect to this average.

Assuming a solution of the form $G_1(\mathbf{r}, \tau) = G_1^o(\mathbf{r}, \tau) \exp(\Phi_s(\mathbf{r}, \tau))$, where $G_1^o(\mathbf{r}, \tau)$ is the solution of the homogeneous correlation diffusion equation and $\Phi_s(\mathbf{r}_s, \mathbf{r}_d, \tau)$ accounts for the scattering of correlation from inhomogeneities. Applying the Rytov approximation,^{24,25} we find the solution of the heterogeneous diffusion equation, i.e.

$$\Phi_s(\mathbf{r}_s, \mathbf{r}_d, \tau) = \frac{-6\mu'_s{}^2 k_o^2 \tau}{G_1^o(\mathbf{r}_s, \mathbf{r}_d, \tau)} \frac{vS}{D_\gamma^{out}} \int d^3r' H(\mathbf{r}', \mathbf{r}_d, \tau) G_1^o(\mathbf{r}_s, \mathbf{r}', \tau) \delta D_B(\mathbf{r}') . \quad (11)$$

$H(\mathbf{r}', \mathbf{r}, \tau)$ is the Green's function for the homogeneous diffusion equation. Measurements of the perturbed temporal field autocorrelation function using several different source-detector pairs can be used along with knowledge of the optical properties and average particle self-diffusion coefficient of the medium to determine $\delta D_B(\mathbf{r})$. The reconstruction is facilitated by inversion of eq. (11). There are many techniques that can be employed to invert eq. (11).²⁴⁻²⁶ Details of our inversion algorithm can be found in O'Leary *et al.*²⁵

Eq. (11) is easily extended to account for spatial variations in the flow of turbid media.

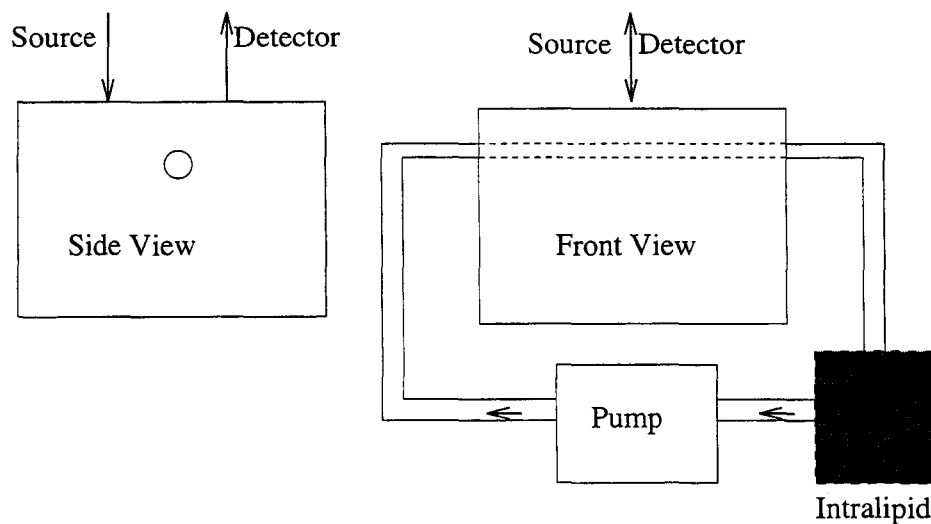


Figure 3: The experimental system is the same as described in fig. 1 except that the TiO_2 slab now has a 6 mm diameter cylindrical cavity instead of a spherical cavity. The cylindrical cavity is centered 13 mm below the surface of the slab and 0.5% Intralipid is pumped through the cavity at flow speeds of 0.442 cm s^{-1} , 0.884 cm s^{-1} , and 1.77 cm s^{-1} . For the solid, $\mu'_s = 4.0 \text{ cm}^{-1}$ and $\mu_a = 0.002 \text{ cm}^{-1}$. For the Intralipid, the optical properties are assumed to be the same as the TiO_2 . The correlation function is measured with the source and detector separated by 2.0 cm, i.e. the source is 1.0 cm to the left of the vein and the detector is 1.0 cm to the right.

4 Experimental Results

4.1 Correlation Scattering from a Spatial Variation in the Brownian Diffusion Coefficient

We demonstrate the scattering of temporal correlation by a dynamical inhomogeneity in an experiment shown in fig. 1. The inhomogeneity is characterized by a contrast in the Brownian diffusion coefficient. In this experiment, the temporal intensity correlation function is measured in remission from a semi-infinite, highly-scattering, solid slab of TiO_2 suspended in resin ($D_B = 0$). The slab contains a spherical cavity filled with a turbid, fluctuating suspension of $0.296 \mu\text{m}$ polystyrene balls ($D_B = 1.5 \times 10^{-8} \text{ cm}^2 \text{ s}^{-1}$).²⁷ In fig. 2 we plot the measured decay of the normalized temporal field correlation function, $g_1(\tau) = \langle E(t)E^*(t + \tau) \rangle / \langle |E|^2 \rangle$, for different source-detector positions and compare these results to theoretical predictions based on eq. (7). The agreement between experiment and theory is good, supporting our view that correlation “scatters” from spatial variations of the particle diffusion coefficient ($D_B(\mathbf{r})$) within the medium. In general, correlation will scatter from spatial variations in the absorption ($\mu_a(\mathbf{r})$), the scattering ($\mu'_s(\mathbf{r})$), and the dynamical ($D_B(\mathbf{r})$, $\Gamma_{eff}(\mathbf{r})$, and $\langle V^2(\mathbf{r}) \rangle$) properties of turbid media.

4.2 Correlation Scattering from Flow in a Cylindrical Vein

The validity of the correlation diffusion equation for systems where the dynamics are governed by shear flow (see fig. 3) is demonstrated in fig. 4. In this experiment, the correlation function is measured in remission from a semi-infinite, highly-scattering, solid slab of TiO_2 suspended in resin ($\Gamma_{eff} = 0$). A 0.5% solution of Intralipid²⁸ is pumped through the cylindrical vein in the slab with pump speeds of 0.442 cm s^{-1} , 0.884 cm s^{-1} , and 1.77

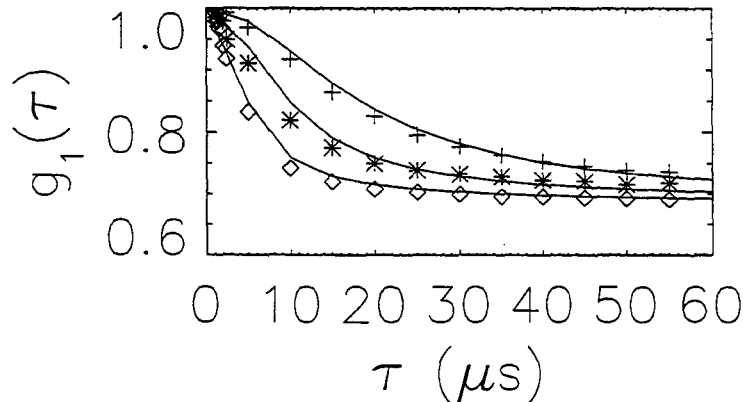


Figure 4: Experimental measurements of the normalized temporal field correlation function for three different flow speeds are compared with theory. Measurements for flow speeds of 0.442 cm s^{-1} , 0.884 cm s^{-1} , and 1.77 cm s^{-1} are indicated respectively by the +’s, *’s, and ◇’s. The solid lines are calculated using the experimental parameters given in fig. 3 and effective shear rates of 3.0 s^{-1} , 6.0 s^{-1} , and 12.0 s^{-1} .

cm s^{-1} . In fig. 4, experimental measurements of the normalized temporal field correlation function are compared with the exact solution of correlation scattering from cylindrical inhomogeneities. The comparison indicates a good agreement between experiment and theory. The parameters used in the calculation, except for Γ_{eff} , are given in fig. 3. The effective shear rate, Γ_{eff} , was determined by fitting the analytic solution to the data with the constraint that Γ_{eff} had to scale linearly with the flow speed. The best fit to the data indicates that Γ_{eff} is approximately 6.8 cm^{-1} times the flow speed. Since the shear rate is given by the change in speed per unit length in the direction perpendicular to the flow, one might expect that the effective shear rate would be the flow speed divided by the radius of the vein. This simple calculation gives an effective shear rate that is a factor of two smaller than the measured Γ_{eff} . This difference will be investigated further in a future publication.

4.3 Image Reconstruction of the Dynamical Properties

In fig. 5 we present an experimental image of $D_B(\mathbf{r})$ for a colloidal sphere contained in a solid resin cylinder of TiO_2 . The cylinder was homogeneous except for a 1.3 cm diameter spherical cavity which was filled with a room temperature aqueous suspension of $0.296 \mu\text{m}$ polystyrene balls and centered at $z=0$ (the z -axis is the axis of the cylinder). Measurements were made every 30° at the surface of the cylinder for $z=0, 1,$ and 2 cm , with source-detector angular separations of 30° and 170° and correlation times of $\tau=15, 25, 35, 45, 55, 65, 75,$ and $85 \mu\text{s}$. Our image of $D_B(\mathbf{r})$ was reconstructed from ~ 600 measurements of the scattered correlation function, $\Phi_s(\mathbf{r}_s, \mathbf{r}_d, \tau)$, using 400 iterations of the Simultaneous Iterative Reconstruction Technique.^{24,25} The $z=0$ slice of the image is shown in fig. 5b. From this image the center (in the x - y plane) of the dynamic region and the magnitude of the particle diffusion coefficient are determined. The center of the object in the image is within 2 mm of the actual center of the dynamic sphere. This discrepancy scales with the uncertainty in the position of the source and detector. The sphere diameter ($\sim 1.3 \text{ cm}$) and particle diffusion coefficient ($\sim 1.8 \times 10^{-8} \text{ cm}^2 \text{ s}^{-1}$) obtained from the imaging procedure also agree reasonably well with experimentally known parameters (1.3 cm and $1.5 \times 10^{-8} \text{ cm}^2 \text{ s}^{-1}$).

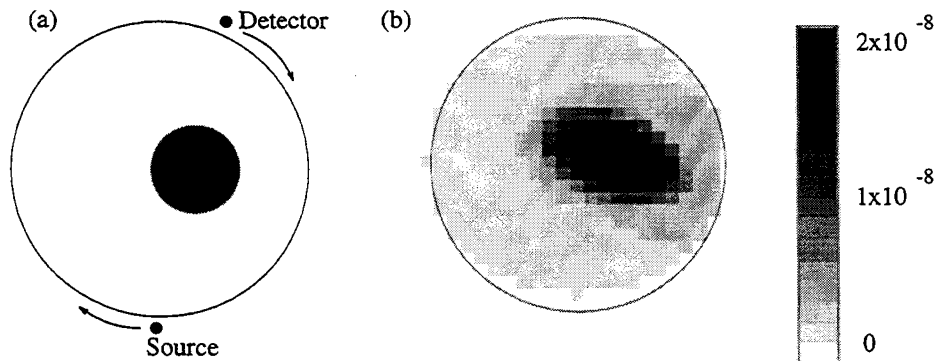


Figure 5: An image reconstructed from experimental measurements of the scattered correlation function is shown in (b). The system was a 4.6 cm diameter cylinder with $\mu'_s=4.0 \text{ cm}^{-1}$, $\mu_a=0.002 \text{ cm}^{-1}$, and $D_B=0$ (see illustration in (a)). A 1.3 cm diameter spherical cavity was centered at $x=0.7 \text{ cm}$, $y=0$, and $z=0$ and filled with a colloid with $\mu'_s=4.0 \text{ cm}^{-1}$, $\mu_a=0.002 \text{ cm}^{-1}$, and $D_B=1.5 \times 10^{-8} \text{ cm}^2 \text{ s}^{-1}$. A slice of the image at $z=0 \text{ cm}$ is presented in (b). The values of the reconstructed particle diffusion coefficients are indicated by the legend in units of $\text{cm}^2 \text{ s}^{-1}$.

5 Conclusion

In conclusion, we have shown that the transport of temporal correlation through heterogeneous turbid media can be viewed as a scattering of diffuse correlation. This concept has been demonstrated experimentally in the context of both forward and inverse problems. We anticipate that these observations will stimulate further studies of dynamical variations in heterogeneous turbid media. In medical optics, for example, this approach offers a simple framework for analyzing the complex signals obtained from fluid flow in the body.

6 Acknowledgments

The authors thank Maureen O'Leary for assistance with the image reconstructions and insightful comments, and acknowledge illuminating conversations with David Pine and Michael Cohen. A.G.Y. acknowledges partial support from the NSF through the P.Y.I. program and grant #DMR93-06814, and the Alfred P. Sloan Foundation. B.C. acknowledges partial support from NS-27346, HL-44125, and CA-50746/60182. I.V.M. wishes to thank the Russian Educational Committee for their support.

7 Appendix

We follow the P_N approximation to reduce the general transport equation to a diffusion equation. The method is simply to expand all angular dependent quantities in a spherical harmonic series and truncate the series at the N^{th} moment.¹³⁻¹⁵ We make the additional assumption that the correlation time is small compared to the time it takes a scattering particle to move a wavelength of light.

The temporal field correlation function and source distribution are expanded as

$$G_1(\mathbf{r}, \hat{s}, \tau) = \sum_{l=0}^N \sum_{m=-l}^l \Gamma_{l,m}(\mathbf{r}, \tau) Y_{l,m}(\hat{s}), \quad (12)$$

and

$$Q(\mathbf{r}, \hat{s}) = \sum_{l=0}^N \sum_{m=-l}^l q_{l,m}(\mathbf{r}) Y_{l,m}(\hat{s}). \quad (13)$$

For the phase function, we make the reasonable assumption that the amplitude is only dependent on the change in direction of the photon and thus

$$\begin{aligned} f(\hat{s} \cdot \hat{s}') &= \sum_{l=0}^{\infty} \frac{2l+1}{4\pi} g_l P_l(\hat{s} \cdot \hat{s}') \\ &= \sum_{l=0}^{\infty} \sum_{m=-l}^l g_l Y_{l,m}^*(\hat{s}') Y_{l,m}(\hat{s}), \end{aligned} \quad (14)$$

where P_l is a Legendre Polynomial and the second line is obtained using the angular addition rule.²⁹ Since $f(\hat{s} \cdot \hat{s}')$ is normalized, $g_0 = 1$.

The single scattering temporal field correlation function for a system of particles undergoing Brownian motion is

$$g_1^s(\hat{s}, \hat{s}', \tau) = \exp\left(-2D_B k_0^2 \tau (1 - \hat{s} \cdot \hat{s}')\right). \quad (15)$$

When $\tau \ll (2D_B k_0^2)^{-1}$, then eq. (15) can be expanded in a Taylor series, which to lowest order is

$$g_1^s(\hat{s}, \hat{s}', \tau) = 1 - 2D_B k_0^2 \tau + 2D_B k_0^2 \tau (\hat{s} \cdot \hat{s}') = 1 - 2D_B k_0^2 \tau + 2D_B k_0^2 \tau \sum_{m=-1}^1 Y_{1,m}^*(\hat{s}') Y_{1,m}(\hat{s}). \quad (16)$$

Note that $(2D_B k_0^2)^{-1} \approx 10^{-3}$ s when $D_B = 1.45 \cdot 10^{-8}$ cm² s⁻¹, the wavelength of light is 514 nm, and the index of refraction is 1.333 and thus the expansion is valid for correlation times less than 100 μ s.

Substituting these expansions into the correlation transport equation, eq. (2), we obtain

$$\begin{aligned} \sum_{l=0}^N \sum_{m=-l}^l \left[\left[\hat{s} \cdot \nabla + \mu_t^{(l)} + g_l k_c \right] \Gamma_{l,m}(\mathbf{r}, \tau) Y_{l,m}(\hat{s}) - q_{l,m} Y_{l,m}(\hat{s}) \right. \\ \left. - k_c \int d\hat{s}' \Gamma_{l,m}(\mathbf{r}, \tau) Y_{l,m}(\hat{s}') \sum_{l'=0}^N \sum_{m'=-l'}^l g_{l'} Y_{l',m'}^*(\hat{s}') Y_{l',m'}(\hat{s}) \sum_{m''=-1}^1 Y_{1,m''}^*(\hat{s}') Y_{1,m''}(\hat{s}) \right] = 0. \end{aligned} \quad (17)$$

New notation is introduced to simplify eq. (17): $\mu_t^{(l)} = \mu_s(1 - g_l) + \mu_a$ is the reduced transport coefficient and $k_c = 2\mu_s D_B k_0^2 \tau$. Remember that the g_l are the coefficients of the Legendre Polynomial expansion of the phase function, therefore $\mu_t^{(0)} = \mu_a$.

Next, we multiply eq. (17) by $Y_{\alpha,\beta}^*(\hat{s})$ and integrate over $d\hat{s}$. The integrals over $d\hat{s}$ and $d\hat{s}'$ are calculated using the orthogonality relations for the spherical harmonics and relations for the integral of three spherical harmonics.³⁰ Integrating for the second, third, and fourth terms of eq. (17) is relatively straightforward. The calculation for the first term is lengthy and clearly documented by Kaltenbach and Kaschke.³¹ The calculation

for the last term is an extension of the calculation for the first term. After calculating the integrals, we arrive at

$$\begin{aligned}
 \mu_i^{(\alpha)} \Gamma_{\alpha, \beta} &+ k_c \Gamma_{\alpha, \beta} \left[g_\alpha - \frac{\alpha}{2\alpha+1} g_{\alpha-1} - \frac{\alpha+1}{2\alpha+1} g_{\alpha+1} \right] \\
 &+ \frac{1}{2} \sqrt{\frac{(\alpha+1-\beta)(\alpha+2-\beta)}{(2\alpha+1)(2\alpha+3)}} \left(\frac{\partial}{\partial x} + i \frac{\partial}{\partial y} \right) \Gamma_{\alpha+1, \beta-1} \\
 &- \frac{1}{2} \sqrt{\frac{(\alpha+\beta)(\alpha+\beta-1)}{(2\alpha+1)(2\alpha-1)}} \left(\frac{\partial}{\partial x} + i \frac{\partial}{\partial y} \right) \Gamma_{\alpha-1, \beta-1} \\
 &- \frac{1}{2} \sqrt{\frac{(\alpha+\beta+2)(\alpha+\beta+1)}{(2\alpha+1)(2\alpha+3)}} \left(\frac{\partial}{\partial x} - i \frac{\partial}{\partial y} \right) \Gamma_{\alpha+1, \beta+1} \\
 &+ \frac{1}{2} \sqrt{\frac{(\alpha-\beta-1)(\alpha-\beta)}{(2\alpha+1)(2\alpha-1)}} \left(\frac{\partial}{\partial x} - i \frac{\partial}{\partial y} \right) \Gamma_{\alpha-1, \beta+1} \\
 &+ \sqrt{\frac{(\alpha+\beta+1)(\alpha-\beta+1)}{(2\alpha+1)(2\alpha+3)}} \frac{\partial}{\partial z} \Gamma_{\alpha+1, \beta} \\
 &+ \sqrt{\frac{(\alpha+\beta)(\alpha-\beta)}{(2\alpha+1)(2\alpha-1)}} \frac{\partial}{\partial z} \Gamma_{\alpha-1, \beta} = q_{\alpha, \beta}. \tag{18}
 \end{aligned}$$

This is a coupled set of linear differential equations for the different moments of the correlation, i.e. $\Gamma_{\alpha, \beta}$.

To obtain the correlation diffusion equation, we neglect all $\Gamma_{\alpha, \beta}$ and g_α for $\alpha > 1$. This assumption is valid when the correlation is nearly isotropic (i.e. the higher moments are negligible) and reduces the infinite set of coupled equations to two, in particular

$$\mu_a \Gamma_0 + k_c \Gamma_0 (1 - g_1) + \nabla \cdot \Gamma_1 = q_{0,0}, \tag{19}$$

and

$$\mu_i^{(1)} \Gamma_1 + k_c \Gamma_1 \left(g_1 - \frac{1}{3} \right) + \frac{1}{3} \nabla \Gamma_0 = 0. \tag{20}$$

We have dropped the azimuthal index for Γ and instead have written the monopole and dipole terms as a scalar and vector respectively. Also, we have assumed that the source is isotropic. By analogy to photon migration, Γ_0 is the fluence of correlation and Γ_1 is the net flux of correlation. Now we solve eq. (20) for Γ_1 and substitute the result into eq. (19). This gives us the desired correlation diffusion equation

$$\left(D_\gamma \nabla^2 - v \mu_a - 2v \mu_s' D_B k_o^2 \tau \right) G_1(\mathbf{r}, \tau) = -v S(\mathbf{r}), \tag{21}$$

where $\Gamma_0(\mathbf{r}, \tau)$ has been replaced with $G_1(\mathbf{r}, \tau)$, $q_{0,0}$ has been replaced with $S(\mathbf{r})$, and $D_\gamma = \frac{v}{3\mu_s'}$ is the *photon diffusion coefficient*. For consistency, μ_a and $k_c(g_1 - 1/3)$ have been dropped from D_γ .

8 REFERENCES

- [1] R. Pecora, *Dynamic Light Scattering: Applications of Photon Correlation Spectroscopy*, Plenum Press, New York, 1985.
- [2] P. N. Pusey and R. J. A. Tough, *Dynamic Light Scattering*, Plenum, New York, 1985.
- [3] P. J. Berne and R. Pecora, *Dynamic Light Scattering* Wiley, New York, 1976.

- [4] See A. Yodh and B. Chance, "Spectroscopy and Imaging with Diffusing Light," *Physics Today*, vol.48, pp.34-40, March 1995, and references therein.
- [5] M. J. Stephen, "Temporal fluctuations in wave propagation in random media," *Phys. Rev. B*, vol.37, pp.1-5, 1988; F. C. MacKintosh and S. John, "Diffusing-wave spectroscopy and multiple scattering of light in correlated random media," *Phys. Rev. B*, vol.40, pp.2382-2406, 1989.
- [6] D. J. Pine, D. A. Weitz, P. M. Chaikin, and Herbolzheimer, "Diffusing-Wave Spectroscopy," *Phys. Rev. Lett.*, vol.60, pp.1134-1137, 1988; G. Maret and Wolf, "Multiple Light Scattering from Disordered Media. The Effect of Brownian Motion of Scatterers," *Z. Phys. B - Condensed Matter*, vol.65, pp.409-413, 1987.
- [7] X. Qiu, X.L. Wu, J.Z. Xue, D.J. Pine, D.A. Weitz and P.M. Chaikin, "Hydrodynamic Interactions in Concentrated Suspensions," *Phys. Rev. Lett.*, vol.65, pp.516-518, 1990; P. D. Kaplan, A. G. Yodh, and D. J. Pine, "Diffusion and Structure in Dense Binary Suspensions," *Phys. Rev. Lett.*, vol.68, pp.393-396, 1992; J.X. Zhu, D.J. Durian, J. Miller, D.A. Weitz, and D.J. Pine, "Scaling of Transient Hydrodynamic Interactions in Concentrated Suspensions," *Phys. Rev. Lett.*, vol.68, pp.2559-2562, 1992; M. H. Kao, A. G. Yodh, and D. J. Pine, "Observation of Brownian Motion on the Time Scale of Hydrodynamic Interactions," *Phys. Rev. Lett.*, vol.70, pp.242-245, 1993; S. J. Nilsen and A. P. Gast, "The influence of structure on diffusion in screened Coulombic suspensions," *J. Chem. Phys.* vol.101, pp.4975-4985, 1994; A. J. C. Ladd, H. Gang, J. X. Zhu, D. A. Weitz, "Time-dependent collective diffusion of colloidal particles," *Phys. Rev. Lett.*, vol.74, pp.318-321, 1995.
- [8] D. J. Durian, D. A. Weitz, and D. J. Pine, "Multiple Light Scattering Probes of Foam Structure and Dynamics," *Science*, vol.252, pp.686-688, 1991.
- [9] H. Gang, A. H. Krall, and D. A. Weitz, "Shape Fluctuations of Interacting Fluid Droplets," *Phys. Rev. Lett.*, vol.73, pp.3435-3438, 1994; P. D. Kaplan, A. G. Yodh, D. F. Townsend, "Noninvasive Study of Gel Formation in Polymer-Stabilized Dense Colloids Using Multiple Scattering Light," *Journal of Colloid and Interface Science*, vol.155, pp.319-324, 1993.
- [10] D. A. Boas, L. E. Campbell, A. G. Yodh, "Scattering and Imaging with Diffusing Temporal Field Correlation," *Phys. Rev. Lett.*, vol.75, pp.1855-1858, 1995.
- [11] B. J. Ackerson, R. L. Dougherty, N. M. Reguigui, and U. Nobbman, "Correlation Transfer: Application of Radiative Transfer Solution Methods to Photon Correlation Problems," *J. Thermophys. and Heat Trans.*, vol.6, pp.577-588, 1992; Dougherty, et al., *J. Quant. Spectrosc. Radiat. Transfer*, vol.52, pp.713, 1994.
- [12] A. Ishimaru, *Wave Propagation and Scattering in Random Media*, Academic Press, New York, 1978.
- [13] K. M. Case and P. F. Zweifel, *Linear Transport Theory*, Addison-Wesley, MA, 1967.
- [14] B. Davison and J. B. Sykes, *Neutron Transport Theory*, Oxford University Press, London, 1957.
- [15] S. Glasstone and M. C. Edlund, *the Elements of Nuclear Reactor Theory*, Edited by D. van Nostrand Co., Princeton N.J., 1952.
- [16] In general the P_1 approximation assumes that the correlation at a given point in space is nearly isotropic. This is a valid assumption when the photons are diffusing. We make the additional assumption that the correlation time is small compared to the time it takes a scattering particle to move a wavelength of light.
- [17] R. Bonner and R. Nossal, "Model for laser Doppler measurements of blood flow in tissue," *Appl. Opt.*, vol.20, pp.2097-2107, 1981.
- [18] X-L. Wu, D. J. Pine, P. M. Chaikin, J. S. Huang, and D. A. Weitz, "Diffusing-wave spectroscopy in a shear flow," *J. Opt. Soc. Am. B*, vol.7, pp.15-20, 1990.

- [19] D. Bicout and R. Maynard, "Diffusing wave spectroscopy in inhomogeneous flows," *Physica A*, vol.199, pp.387-411, 1993; D. Bicout and G. Maret, "Multiple light scattering in Taylor-Couette flow," *Physica A*, vol.210, pp.87-112, 1994; D. J. Bicout and R. Maynard, "Multiple light scattering in turbulent flow," *Physica B*, vol.204, pp.20-26, 1995.
- [20] R. C. Haskell, L. O. Svaasand, T. Tsay, T. Feng, M. S. Adams, and B. J. Tromberg, "Boundary conditions for the diffusion equation in radiative transfer," *J. Opt. Soc. Am. A*, vol.11, pp.2727-2741, 1994.
- [21] The sphere is centered on the origin, and the source is placed on the z-axis to exploit azimuthal symmetry.
- [22] D. A. Boas, M. A. O'Leary, B. Chance, and A. G. Yodh, "Scattering of Diffuse Photon Density Waves by Spherical Inhomogeneities within Turbid Media: Analytic Solution and Applications," *Proc. Natl. Acad. Sci. USA*, vol.91, pp.4887-4891, May 1994; P. N. den Outer, T. M. Nieuwenhuizen, and A. Lagendijk, "Location of Objects in Multiple-scattering Media," *J. Opt. Soc. Am. A*, vol.10, pp.1209-1218, 1993; S. C. Feng, F. A. Zeng, and B. Chance, "Photon migration in the presence of a single defect - A perturbation analysis," *Appl. Opt.*, vol.34, pp.3826-3837, 1995.
- [23] H. C. van de Hulst, in *Light Scattering by Small Particles*, Dover Publications Inc., NY, 1981.
- [24] A. C. Kak and M. Slaney, *Principles of Computerized Tomographic Imaging*, IEEE Press, New York, 1988.
- [25] M. A. O'Leary, D. A. Boas, B. Chance, and A. G. Yodh, "Experimental images of heterogeneous turbid media by frequency-domain diffusing-photon tomography," *Optics Letters*, vol.20, pp.426, 1995.
- [26] See related works by S.R. Arridge *et al.*, J.P. Kaltenebach *et al.*, and R.L. Barbour *et al.*, in the volume "*Medical Optical Tomography: Functional Imaging and Monitoring*", G. Muller *et al.*, SPIE Optical Engineering Press, Bellingham, WA, Vol. 1s11, pp. 31-143, 1993.
- [27] Due to the non-ergodic nature of the system, it was necessary to ensemble average the correlation function by translating the sample over a 400 μm region during each measurement of the correlation function. See J.Z.Xue, D.J.Pine, S.T.Milner, X.L.Wu, and P.M.Chaikin, "Nonergodicity and Light Scattering from Polymer Gels," *Phys. Rev. A*, vol.46, pp.6550-6563, 1992 for further discussion of this procedure.
- [28] Intralipid is a polydisperse suspension of fat particles ranging in diameter from 0.1 μm to 1.1 μm . The Intralipid used here was obtained from the Hospital of the Univ. of Penn.
- [29] J. D. Jackson, *Classical Electrodynamics*, Wiley & Sons Inc., New York, Chap. 3 & 16, 1975.
- [30] G. B. Arfken, *Mathematical Methods for Physicists*, Academic Press Inc., Orlando, Chap. 12.9, 1985.
- [31] J. M. Kaltenebach and M. Kaschke, *Frequency and Time Domain Modelling of Light Transport in Random Media*, SPIE .